Quantum Electronics **32** (9) 756 – 764 (2002)

REVIEW

PACS numbers: 63.22.+m; 72.10.Di; 78.66.Bz
DOI: 10.1070/QE2002v032n09ABEH002288

Trapped phonons in ultrathin metal films: the interpretation of recent femtosecond experiments

A.O. Melikyan, H.R. Minassian

***Abstract*. The results of recent experimental and theoretical studies of the nonequilibrium dynamics of electrons and phonons excited by femtosecond laser pulses in ultrathin metal films are discussed. Experimental data obtained by the femtosecond pump – probe wave (FPPW) method are analysed using a two-temperature model and non-thermal models. A key role of the size quantisation of a phonon spectrum in the dynamics of phonons and electron – phonon interaction is substantiated. The application of the FPPW method in superconductivity studies is also discussed.**

Keywords: *femtosecond pulse, ultrathin film, size quantisation, electron – phonon interaction.*

1. Introduction

At present the technology of preparation of ultrathin films has reached its theoretical limit, providing the fabrication of one atom thick films. The physical properties of such films strongly differ from those of bulky samples, and it seems that all the differences can be explained only in the future. The experimental studies of ultrafast processes in films, which are of most interest, became possible due to the development of the methods for generating femtosecond laser pulses of a given duration in different spectral regions.

Interest in ultrathin metal films and extensive studies of their properties are caused by the application of these films as contacts in fast electronic and optoelectronic devices. Obviously, the response time of such devices is determined by the relaxation time of the electron subsystem. It was shown already in the first experiments with femtosecond pulses that the relaxation time depends on the film thickness, increasing in thin films and thereby deteriorating the response time. The study of the mechanism of this effect is of much current interest both for the theory and applications.

The definition of a film should be specified. Whether or not a particular sample can be called a film is determined by its properties being studied. If, for example, we are interested in the conductivity of a metal sample, this is determined by the dependence of the sample resistance on its thickness due to diffusion scattering of carriers from the surface roughness, whose contribution in thin films becomes comparable with those from usual resistance mechanisms. In this case, an important parameter is the electron mean free path determined by scattering of electrons by impurities and lattice vibrations.

We discuss in this review the studies of processes proceeding in thin metal films irradiated by femtosecond laser pulses. One should bear in mind that, as a rule, very thin films are prepared by the deposition of atoms on a substrate, which can substantially affect the development of processes under study. As expected, when the film thickness exceeds the electron mean free path, hot electrons relax as in a bulky sample. A criterion for determining whether or not a sample can be treated as a film with respect to purely phonon processes, such as thermal expansion and sound propagation, depends on the substrate properties and is discussed in Section 5.

The question about the role of a size quantisation of the electron spectrum in a film is solved as follows. There exist two characteristics lengths: the mean free path $l_{\rm fp}$ and the de Broglie wavelength $\lambda_{\rm B}$. If $l_{\rm fp} \leqslant \lambda_{\rm B}$, irrespective of the film thickness, the size quantisation effects are insignificant because of a strong broadening of the energy levels. If the opposite inequality $l_{\rm fp} \geqslant \lambda_{\rm B}$ is satisfied, a coherent state of an electron is conserved over the de Broglie wavelength and more, and, when the film thickness is comparable with $\lambda_{\rm B}$, the size quantisation comes to play. For example, in typical semiconductors with the effective mass of carriers in the conduction band, which is approximately ten times smaller than the mass of a free electron, the de Broglie wavelength of electrons at room temperature is $\sim 10-100$ nm; therefore, the electron size quantisation effects become essential when the film thickness is comparable with this value.

The de Broglie wavelength of electrons in metals is of the order of 0.1 nm. Nevertheless, we will show below that the size quantisation affects the electron – phonon interaction in metal films of thickness 10 nm, but now due to quantisation of the phonon spectrum. However, when the film thickness is such that the distance between the electronic levels of the size quantisation exceeds the Debye frequency of the metal and emission of phonons by electrons is strongly hindered, the role of size quantisation of electrons becomes very important.

Unlike, metal films, the size quantisation of the phonon spectrum and its effect on the electron – phonon interaction in semiconductor films have been well studied.

A.O. Melikyan, H.R. Minassian State Engineering University of Armenia, ul. Teryana 105, 375009 Erevan, Armenia; e-mail: shen@armico.com; web site: www.seua.am

Received 5 April 2002
Kvantovaya Elektronika **32** (9) 756 – 764 (2002)
Translated by M.N. Sapozhnikov

2. Review of experiments

The ultrafast dynamics of nonequilibrium electrons in metals have been recently studied in many papers [1 – 10]. The most advanced experimental method for investigating these processes is based on the irradiation of a sample by two femtosecond laser pulses separated by a time delay. The first pulse serves as a pump pulse, while the second pulse probes variations induced by the pump pulse in the sample. This method is called the femtosecond pump – probe wave (FPPW) method. It involves the measurement of the reflection coefficient R of a probe pulse as a function of the delay time between the pump and probe pulses.

It was shown in a number of recent experiments that excitation of electrons in ultrathin metal films by femtosecond laser pulses leads to the nonequilibrium dynamics of electrons and their non-thermal transport [1 – 11]. These two processes cause a change in the reflection coefficient of the film due to a change in the concentration of charges in a surface layer of thickness equal to the depth of penetration of light to the metal (this layer is called sometimes a skin layer). Two pump pulses separated by a time delay can be also used, which can provide a more detailed information on the dynamics of hot electrons [12]. When both pulses are incident on the same surface of a metal film (copropagating pulses), the reflection coefficient of the probe pulse gives information only on the relaxation times of hot electrons. If the pulses are incident on the opposite surfaces of the film (counterpropagating pulses), we can obtain an additional information on the electron transport.

Beginning from the first FPPW experiments performed in the mid-1980s, the dependence of the reflection coefficient of the probe pulse on the film thickness was observed. Below, we present the results of experiments with copropagating ([5], Fig. 1; [11], Fig. 2) and counterpropagating pulses ([10], Fig. 3), which demonstrate this dependence for films of thickness smaller than 100 nm. The results obtained with copropagating pulses clearly show that the reflection coefficient R relaxes nonexponentially (linearly) at delay times smaller than 7 ps in 10-nm thick films and less than 1 ps in 50-nm thick films.

New experimental data on the dynamics of thermal expansion, which were obtained by the modified FPPW method, are presented in paper [13]. The authors of this paper investigated vibrations in an ultrathin nickel film excited by femtosecond pulses. They showed that the propagation velocity of a thermal-expansion pulse decreased with decreasing film thickness. The vibrational modes and thermal expansion of the ultrathin nickel film on a copper substrate could be detected due to the surface sensitivity of the SHG in a centrally symmetric medium. In these experiments, 800-nm, 150-fs pulses were incident on the nickel film and excited the d electrons, which was accompanied by excitation of vibrational modes in the film, resulting in its thermal expansion.

The mechanism of the detection of these processes can be described as follows. The dispersion of the d electrons in nickel decreases due to thermal expansion of the film caused by pumping, which is equivalent to an increase in the density of states. This in turn results in the amplification of the SHG signal caused by the probe pulse, which follows the pump pulse with a certain delay. The subsequent measurement of the intensity of the SHG signal as a function of the delay time gives information on the vibrations and thermal expansion of the film. The ratio of the pump and probe pulse intensities was 20 : 1, so that the probe pulse did not

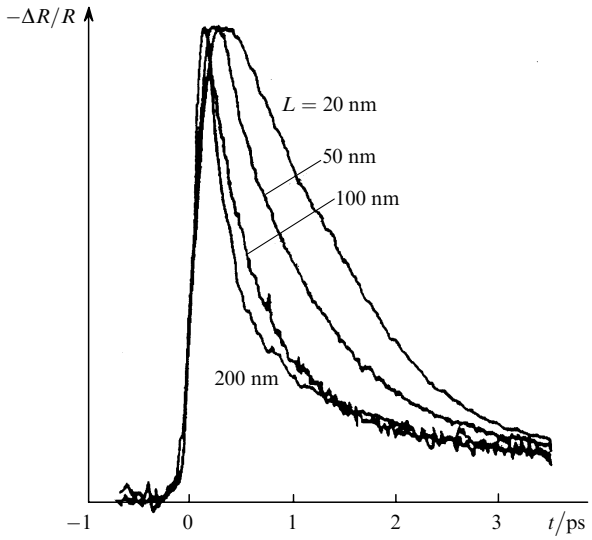

Figure 1. Dependences of the relative change in the reflection coefficient $-\Delta R/R$ on the delay time t between the pump and probe pulses incident on the same surface of the film. The relaxation time of R decreases with increasing film thickness L up to 100 nm; above 100 nm, the change is very small.

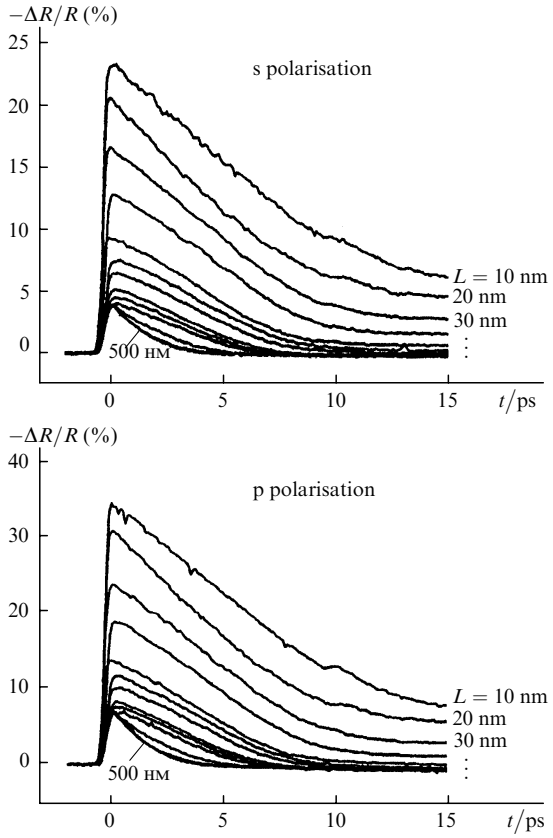

Figure 2. Dependences of the relative change in the reflection coefficient $-\Delta R/R$ on the delay time t between the pump and probe pulses incident on the same surface of the film for the s and p polarisations, a pulse duration of 100 fs, a wavelength of 500 nm, and different thicknesses L of the film; between 10 and 100 nm, the film thickness was changed by a step of 10 nm, then 200, 300, and 500-nm thick films were measured.

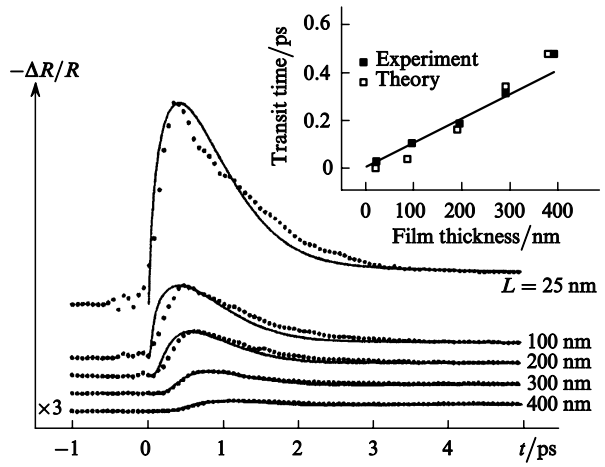

Figure 3. Dependences of the relative change in the reflection coefficient $-\Delta R/R$ of a single crystal gold film on the delay time t between the pump and probe pulses incident on the opposite surfaces of the film. For negative times, all the curves coincide (they are displaced relative to each other for clarity). The scale of the curve for the 400-nm thick film is different. The inset shows the dependence of the time for which a change in R on the opposite side of the film reaches 15 % of its maximum value on the film thickness (calculations were performed assuming that the diffusion motion of electrons).

excite any additional vibrations. It was shown [13] that the intensity of the SHG signal caused by the probe pulse oscillates as a function of the delay time; however, no oscillations were observed in films of thickness exceeding six atomic layers. This is explained by a strong dissipation of the vibrational energy. Another peculiarity is a decrease in the sound speed with decreasing film thickness (Fig. 4).

These properties suggest that, to explain the dependence of the relaxation time of electrons and the sound speed on the film thickness, it is necessary to analyse carefully the experimental data available and to obtain new data.

3. Available models

The first attempt to interpret experimental data was based on the two-temperature model (TTM) [14]. It was assumed that excited electrons could be described by the so-called hot Fermi distribution with a temperature different from the lattice temperature. This assumption is valid if a hot Fermi distribution is formed much faster than the electron gas has time to transfer a noticeable amount of its energy to the lattice. The electron gas is thermalised due to electron–electron scattering and inelastic processes of the Auger recombination type. Although the TTM can describe quantitatively some features of the electron relaxation, the conditions of its applicability are not completely satisfied in FPPW experiments [8–13, 15], and more general methods were proposed based on the Fermi liquid theory [16]. In particular, the authors of paper [15] neglected, within the framework of this theory, the reverse influence of the energy transfer from electrons to a lattice on the kinetics of the electron–electron interaction. They obtained good agreement between the calculated acoustic response of a thin (62.4, 73.2, and 93.3 nm thick) aluminium film excited by femtosecond laser pulses and experimental data. Because the film thickness was comparable with the electron free path, the acoustic pulse appeared due to energy transfer from electrons to a lattice, followed by thermal expansion. Note, however, that the acoustic response cannot provide complete information on the kinetics of interacting electrons and phonons.

To explain a rather long relaxation 'tail' observed in paper [8], a phenomenological term describing reverse energy transfer from a lattice to electrons was introduced into kinetic equations of the Fermi liquid theory [10]. However, as noted in paper [17], a similar term is present in TTM equations as well.

Two-temperature model. According to this model, the rate of energy transfer from electrons to a lattice is described by the expression [14]

$$U = B\left[\left(\frac{T_e}{T_D}\right)^5 \int_0^{T_D/T_e} \frac{x^4 dx}{e^x - 1} - \left(\frac{T_{lat}}{T_D}\right)^5 \int_0^{T_D/T_{lat}} \frac{x^4 dx}{e^x - 1}\right], \quad (1)$$

where T_e and T_{lat} are the electron and lattice temperatures, respectively; T_D is the Debye temperature; and B is a temperature-independent coefficient. As shown in [14], at high temperatures (T_{lat}, $T_e \gg T_D$), the rate U takes the form

$$U = g(T_e - T_{lat}), \quad (2)$$

which is commonly used, where g is a constant of the electron–phonon interaction. It can be easily shown, however, that the next term of the expansion in powers of the ratios T_D/T_{lat} and T_D/T_e is small even when T_{lat} and T_e are approximately equal to T_D, so that expression (2) is valid within a rather broad range. By using (2), we can obtain macroscopic energy balance equations

$$C_e(T_e)\frac{dT_e}{dt} = K\frac{d^2T_e}{d^2z} - g(T_e - T_{lat}) + P, \quad (3)$$

$$C_{lat}\frac{dT_{lat}}{dt} = g(T_e - T_{lat}), \quad (4)$$

where C_e and C_{lat} are the heat capacities of the electron gas and lattice, respectively; K is the heat conduction; and P is the absorbed power density. By solving these equations and comparing the results with the experimental data, we can estimate the relaxation times of hot electrons and some other important parameters of the process. In particular, as shown in [11], when the reflection coefficient is directly proportional to the absolute temperature, equations (3) and (4) confirm a linear law of relaxation of R for film of thickness less than 100 nm during a few picoseconds after the pump pulse propagation (Fig. 2). Indeed, at the very beginning of energy transfer, but after propagation of the pump pulse, whose duration was 150 fs, the inequality $T_e \gg T_{lat}$ is valid. In the case of thin films, we can also neglect the diffusion term. In addition, because at temperatures low compared to the degradation temperature the electron heat capacity can be written as $C_e(T_e) = AT_e$, where A is a constant, which is known for each metal, and the lattice heat capacity is constant at temperatures above the Debye temperature, we obtain from equation (3) that $T_e(t) = T_{e\,max} - (g/A)t$. The slope of the straight line gives the electron–phonon interaction constant g. For example, $g = (2.1 - 2.6) \times 10^{10}$ W cm^{-1} K^{-1} for 10–100-nm thick

gold films at wavelengths 540 – 546 nm [13]. This value is close, within accuracy of ±10 %, to the values obtained by other methods [6 – 9].

Non-thermal models. As shown in paper [7], a quasi-equilibrium temperature is established in the electron subsystem upon femtosecond excitation for the time exceeding at least 0.6 ps. We suppose that in this case the conditions of applicability of the TTM are not satisfied and the TTM cannot describe the very beginning of the process of energy transfer between electrons and the lattice, which proceeds during the first picosecond after excitation. This stimulated the development of non-thermal models based on the kinetics of electron – electron and electron – phonon interactions, similarly to the Fermi liquid theory.

Thus, the authors of paper [15] assumed that excited electrons are scattered by electrons located below the Fermi level E_F, whereas collisions between excited electrons are insignificant for thermalisation. Then, the time dependence of the number of excitations $n(E)$ with the energy E is described by the expression

$$\frac{dn(E,t)}{dt} = -\frac{n(E,t)}{\tau_0}\frac{E^2}{E_F^2} + 6\int_E^\infty \frac{dE'}{E_F}\frac{E'-E}{E_F}\frac{n(E',t)}{\tau_0}, \quad (5)$$

where

$$\tau_0 = \frac{128}{\pi^2\sqrt{3}\omega_p}; \quad (6)$$

and ω_p is the plasma frequency. The first term in the right-hand side of (5) describes the electrons leaving the state with the energy E after their scattering from a screened Coulomb potential of unexcited electrons. The factor E^2/E_F^2 appears, as is shown in the Fermi liquid theory, due to consideration of the Pauli principle. The second term in the right-hand side of (5) describes the electrons undergoing transitions to this state.

Expression (6) was obtained in the approximation of a high-density electron gas. The rate of energy transfer to the lattice is proportional to the number of excitations. By using this theory, the authors of paper [15] studied the acoustic response of a thin $\sim 60 - 90$-nm thick aluminium film excited by a femtosecond laser pulse and found good quantitative agreement with experimental data for delay times up to 60 ps, without any fitting parameters. However, as mentioned above, the acoustic response does not give a complete information on the process kinetics.

The authors of paper [10] assume that a change in the reflection coefficient is caused by hot electrons produced in a thin gold film by pumping. A rather long relaxation tail was observed in films of different thicknesses. To explain anomalous long relaxation times, the authors [10] introduced a phenomenological parameter S describing reverse energy transfer from the lattice to electrons. The evolution of the number of excitations is described by the equation

$$\frac{dn(E,t)}{dt} = -\frac{n(E,t)}{\tau_0}\frac{E^2}{E_F^2} + 6\int_E^\infty dE'\frac{E'-E}{E_F^2}\frac{n(E',t)}{\tau_0} - \frac{Qn(E,t)}{\langle E\rangle} + S\frac{Qn_p(E,t)}{\hbar\Omega_{av}}, \quad (7)$$

where Q is the rate of energy transfer from quasi-particles to the lattice; $\langle E\rangle$ is the average energy of quasi-particles; Ω_{av} is the average energy of acoustic phonons; and $n_p(E,t)$ is the number of phonons.

The quantity S plays the role of a fitting parameter. The dispersion of values of S providing agreement with the experimental data for films of thickness 25 – 400 nm was 15 %. In addition, the data obtained in paper [15] favour the ballistic flight of electrons through the film (see inset in Fig. 3). However, the electron transport velocity (velocity of the ballistic flight) equal to $\sim 1.06 \times 10^6$ m s^{-1} proved to be, according to measurements [10], lower than the velocity of electrons on the Fermi surface equal to $\sim 1.4 \times 10^6$ m s^{-1}. We will show in Section 4 that the size quantisation of the phonon spectrum favours a collisionless flight of electrons through the film.

It is important to note that the last term in (7), which provides the agreement with experimental data, plays the same role as the term T_{lat} in equation (3) (both these terms are positive). That is why both the TTM and the non-thermal theory [10] almost identically describe the behaviour of the reflection coefficient at long times. At the same time, a main disadvantage of the kinetic approach based on the Fermi liquid theory [equation (5)] compared to the TTM – a neglect of energy transfer from phonons to electrons, becomes evident.

However, all the theories considered above neglect the influence of the size quantisation of phonons on the dynamics of electron – phonon interaction. It is obvious that this effect can be observed only when the uncertainty of the electron energy upon electron – electron scattering is smaller than the interval of the size quantisation of the phonon spectrum. In other words, this effect becomes dominant when the film thickness is smaller than the electron mean free path during electron – electron scattering, i.e., smaller than 100 nm [17].

Unlike metal films, the effects of size quantisation in semiconductor films are well studied both theoretically and experimentally, which was stimulated by numerous applications of these films [18]. Both electron and phonon spectra are quantised in semiconductor films. The electron – phonon [19] and electron – photon [20] interactions in films strongly differ from these interactions in bulky samples, mainly due to specific restrictions imposed by the laws of conservation of energy and momentum. This results in noticeable changes in the relaxation rate of electrons, affecting the working parameters of semiconductor electronic devices [21, 22]. From this point of view, the consideration of the effects of size quantisation in the theory of processes proceeding in ultrathin metal films is very important, especially as the fabrication of 1 – 4 atomic layers thick films is already possible [13, 23].

4. Trapped phonons

The behaviour of electrons, phonons, excitons and other quasi-particles in thin solid films differs from their behaviour in bulky samples. This is explained by the fact that, because of the boundary conditions imposed on the wave function of a quasi-particle, its wave vector directed perpendicular to the film surface takes discrete values, resulting in a strong rearrangement of the frequency and energy spectra, as well as in a peculiar dependence of the quasi-particle energy on the film thickness. This resembles the situation when a particle is localised in a quantum well (quantum trapping). In the case of quasi-particles, this

effect is called the size quantisation [19]. For example, when the boundaries of a thin film impose the restriction on the phonon movement (phonon trapping), the size quantisation of their frequency spectrum leads to the dependence of the matrix element of the electron–phonon interaction on the film thickness and to some kinematic restrictions (also depending on the film thickness) in the laws of conservation of energy and momentum [17].

As shown in paper [17], the size quantisation in a metal film can substantially reduce the probability of electron–phonon scattering. The influence of the size quantisation becomes obvious, for example, at very low temperatures. The matter is that the phonon spectrum of a film has a nonzero lower boundary

$$\omega_{\min} = \frac{a\omega_{\max}}{2}\frac{\pi}{L}, \tag{8}$$

where a is the interplane distance; $\omega_{\max}$ is the maximum frequency of the phonon spectrum, the value of $(1/2)a\omega_{\max}$ being coincident with the sound speed v_s in a bulky sample; and L is the film thickness. This gives the probability of the electron–phonon scattering at low temperatures

$$W \propto \frac{W_{\text{bulk}}}{\exp(\hbar\omega_{\min}/kT) - 1}, \tag{9}$$

where W_{bulk} is the probability of scattering in a bulky sample. For a 10-nm thick film, the sound speed 3×10^3 m s^{-1}, and temperature 10 K, the dominator in (9) becomes very large, and we have $W \ll W_{\text{bulk}}$. Note that the scattering probability W_{bulk} depends on the film thickness because the latter determines $\omega_{\min}$ in terms of the minimum phonon frequency.

At room temperature and for the same values of other parameters, the exponent will be much smaller than unity, and the dependence on the film thickness will be retained; however, another factor should be also taken into account, namely, a finite mean free path of electrons due to electron–electron scattering. It follows from the numerical calculation (see Fig. 1 in [17]) that, when both these factors are taken into account, the probability of electron–phonon scattering noticeably decreases with decreasing film thickness. When $L > \Lambda$, where Λ is the electron mean free path, W is well approximated by the expression

$$W = W_{\text{bulk}}\left[1 - \exp(-L/\Lambda)\right]. \tag{10}$$

One can see from (8) and (9) that the electron–phonon coupling constant depends on the film thickness, which should be taken into account in the theory of kinetic effects in metal films. It is obvious that ultrathin films are most suitable objects for the experimental confirmation of size quantisation because they exhibit distinct discrete spectra. Moreover, effects destroying coherence (for example, diffusion) are negligible in ultrathin films. It is also important that, in order to observe the size quantisation of a phonon spectrum, the observation time should exceed the time L/v_s of flight of a phonon from one boundary of the film to another. The frequency spectrum of a trapped phonon is formed for this time. For the sound speed equal to 2×10^3 m s^{-1} and a 10-nm thick film, this time is ~ 5 ps. It seems that this effect was observed in paper [11], where the dependence of the reflection coefficient of a probe pulse on the film thickness was observed only for delay times of the probe pulse with respect to the pump pulse exceeding 5 ps. It is clear that the relaxation times also should be longer than the transit time of a phonon.

5. Quantised acoustic phonons in an ultrathin nickel film

To observe trapping of phonons in metal films, it is by no means necessary to study the electron–phonon interaction. This effect was recently demonstrated in FPPW experiments [13] with nickel films of thickness from 40 to 1 nm on a copper substrate when the dependence of the sound speed on the film thickness was observed in the quantisation direction (001) (see Fig. 27 in [11]). This phenomenon can be interpreted as phonon trapping, as we will show below (see also [24]).

An acoustic pulse propagates in a medium at a velocity equal to the group velocity of phonons

$$v_g = \frac{\partial\omega}{\partial q} = \frac{1}{2}\omega_{\max}a_1\cos\left(\frac{qa_1}{2}\right), \tag{11}$$

where q is the wave vector in the direction (001) and a_1 is the interplane distance in the direction (001). In the case of size quantisation, expression (11) for the group velocity should be changed because the phonon spectrum is discrete. Indeed, in a simplest case, when only two waves are excited with close frequencies ω_1 and ω_2 and wave vectors q_1 and q_2, the maximum of the wave packet propagates at the velocity

$$v_g = \frac{\omega_2 - \omega_1}{q_2 - q_1}. \tag{12}$$

The spectrum of a bulky sample is continuous, and the ratio of finite differences in (12) transforms to a derivative, as in (11). Let us find now the phonon spectrum under conditions of size quantisation when a film is deposited on a substrate. Let us denote an atomic layer adjacent to a substrate by the subscript 1 and the displacement of the v layer by u_v. The subscript $v = 0$ corresponds to an immobile atomic layer of the substrate directly adjacent to the film, i.e., $u_0 = 0$. The displacements are described by equations

$$\begin{aligned} m\ddot{u}_1 &= -ku_1 + k(u_2 - u_1), \\ m\ddot{u}_v &= -k(2u_v - u_{v+1} - u_{v-1}), \qquad v > 1, \end{aligned} \tag{13}$$

and the boundary condition has the form

$$u_{N+1} = u_N.$$

Here, N is the number of atomic layers and k is the force constant. We can calculate the phonon spectrum by neglecting a small difference between the force constants $k_{\text{Ni–Ni}} = 37.90$ kg s^{-2} and $k_{\text{Ni–Cu}} = 33$ kg s^{-2} [13], which causes a very small frequency shift. Another important approximation is the neglect of the energy flow to the substrate. It is known that the energy loss results in the

appearance of the imaginary part of the frequency, which determines the linewidth.

We see a solution of system (13) in the form

$$u_v = u\sin(v\varphi)\exp(-\mathrm{i}\omega t). \tag{14}$$

We find the phase shift φ from the second boundary condition $\sin(N\varphi) = \sin[(N+1)\varphi]$, which gives

$$\varphi_n = \frac{2n-1}{2N+1}\pi. \tag{15}$$

The frequency spectrum is found by substituting the solution (14) to system (13) and taking into account (15):

$$\omega_n = \omega_{\max}\left|\sin\left(\frac{2n-1}{2N+1}\,\frac{\pi}{2}\right)\right|, \quad n = 1, 2, 3,...,N. \tag{16}$$

One can see from (11) and (16) that the dependence of the group velocity on the film thickness for $n \ll N$ is determined by the expression

$$v_{\mathrm{g}}(L) \simeq v_{\mathrm{bulk}}\left(1 - \frac{\pi^2 n^2 a_1^2}{8L^2}\right), \quad v_{\mathrm{bulk}} = \frac{\omega_{\max} a_1}{2}, \tag{17}$$

where v_{bulk} is the group velocity in a bulk sample. It follows from (17) that the group velocity decreases with decreasing film thickness.

Note that the minimum frequency in the case of four layers, i.e., for $N = 4$ and $n = 1$, calculated in [24] from (16) well agree with the value 1.4 THz measured in [13]. Indeed, by substituting the values of parameters $v_{\mathrm{bulk}} = 4200$ m s^{-1} and $a_1 = 0.17$ nm from [13] into (16) and taking into account (17) we obtain the frequency equal to ~ 1.39 THz.

On the axes in Fig. 27 from [13] (see also Fig. 4 in this paper) the film thickness and the time of appearance of the first maximum of the second harmonic of the probe pulse are plotted. The experimental data for films of thickness above 20 atomic layers (~ 4 nm) are well fitted by a straight line, whose slope corresponds to the sound speed in a bulk sample (4200 m s^{-1}). In films of a lower thickness, a decrease in the sound speed is observed, which agrees qualitatively with (17). This circumstance clearly demonstrates that the group velocity of acoustic phonons was indeed measured in the experiment. Therefore, the experimental data should correspond to a curve described by the equation

$$\frac{L}{v_{\mathrm{g}}(L)} = \tau, \tag{18}$$

where τ is the time of propagation of an acoustic phonon from the fixed surface of the film to its free surface. Of course, the measured value of L/τ decreased with decreasing film thickness.

We will interpret these data quantitatively using expressions (12), (16), and (18). The best agreement with the measured values is obtained by assuming that the fourth and fifth phonon modes are most important (this assumption is substantiated in Section 6), which gives

$$v_{\mathrm{g}} = \frac{\omega_5 - \omega_4}{q_5 - q_4} = \frac{2v_{\mathrm{s}}}{\pi}(2N+1)\sin\left(\frac{\pi}{4N+2}\right)\cos\left(\frac{4\pi}{2N+1}\right). \tag{19}$$

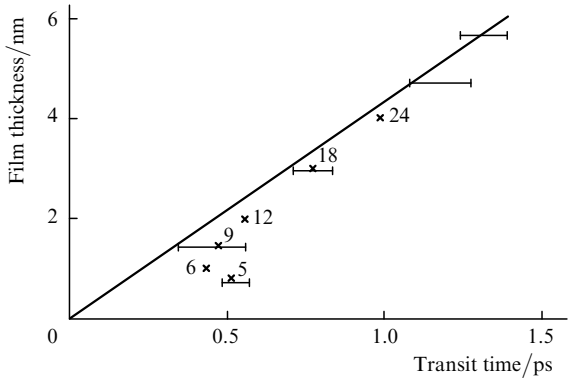

Figure 4. Relation between the film thickness and the transit time of an acoustic signal through the film. The solid straight line corresponds to the sound speed in a bulky sample; the horizontal bars are experimental data; crosses correspond to the values calculated in [24]; the figures are the numbers of atomic layers in a sample.

Fig. 4 shows that the values calculated from (18) and (19) well agree with the experimental values. One can see that the crosses approach the straight line with increasing number of atomic layers, i.e., the group velocity in insensitive to the film thickness for $n \leqslant 5$.

According to the results of measurements [13], vibrations in a film four atomic layer thick decay exponentially with the decay time 1.6 ps, which we attribute to the energy leakage to the substrate. This means that phonon bands should have the width ~ 0.6 THz. This value is very close to the value obtained from the Fourier analysis of experimental data (inset in Fig. 24 in [13]). When the difference of frequencies of adjacent modes becomes comparable with this width, the film begins to behave as a bulky sample with respect to the effect under study. Indeed, by using the values of parameters mentioned above ($\omega_{\max} \sim 8$ THz), we obtain

$$\omega_5 - \omega_4 = \frac{4\pi}{N}\,[\mathrm{THz}],$$

and by equating this value to the width, we find $N \approx 20$, which agrees with the results of measurements presented in Fig. 4.

Therefore, phonon trapping is manifested not only in the electron – phonon interaction but also noticeably affects the propagation of acoustic waves in ultrathin films.

6. Dynamics of thermal expansion of an ultrathin film

To describe the thermal expansion of a film upon excitation of lattice vibrations, it is sufficient to take into account the lowest-order anharmonic terms [25]

$$\ddot{u}_v + \frac{k}{m}(2u_v - u_{v+1} - u_{v-1})$$

$$= \alpha\left[(u_{v+1} - u_v)^2 - (u_v - u_{v-1})^2\right] + f(t), \tag{20}$$

in equations for the displacements of ions. Here, u_v is the displacement of the (001) crystal plane with the subscript 1 as a whole, the plane with the subscript 1 being adjacent to a substrate; the function $f(t)$ describes excitation of

vibrations by a pump pulse interacting with the d electrons; and α is the anharmonicity constant.

The function $f(t)$ is related to the recoil of ions during a transition of the d electrons to the conduction band upon pumping [26]. It is assumed that the transport of electrons through an ultrathin film is ballistic [6, 8–10], so that no vibrations are excited after the propagation of a pump pulse.

Therefore, the function $f(t)$ is nonzero only during the propagation of the pump pulse. The boundary conditions remain the same as in Section 4, i.e., we still neglect the transfer of vibrational energy to the substrate. This approximation is justified by the fact that a nickel film expands upon heating much more rapidly than a copper substrate [13]. In the zero-order approximation over the anharmonicity constant, the solution of system (20) has the form

$$u_v^{(0)} = \sum_n \left[\frac{1}{ma_N\omega_n} \int_{-\infty}^{t} f(t') \sin\omega_n(t-t')\mathrm{d}t' \times \sin(\varphi v) \sum_{v'} \sin(\varphi v') \right] + u_{vn}^{(0)}, \tag{21}$$

where

$$a_N = \sum_v \sin^2\left(\frac{2n-1}{2N+1}\pi v\right) = \frac{2N+1}{4}$$

is the normalisation factor for the nth mode. The last term in the right-hand side is the solution of the corresponding homogeneous equation in the zero-order approximation over anharmonicity and describes thermal vibrations of the lattice before their excitation by the pump pulse. The duration of the pump pulse in experiments [13] was 150 fs, whereas the observation was performed for a few picoseconds after the end of the pump pulse. Therefore, the upper limit of the integral in (21) can be replaced by infinity, and the solution takes the form

$$u_v^{(0)} = \sum_n c_{vn} \sin\omega_n t, \tag{22}$$

where c_{vn} is determined from (21) for $t \to \infty$. This expression should be substituted into the first-order approximation equation

$$\ddot{u}_v^{(1)} + \frac{k}{m}\left(2u_v^{(1)} - u_{v+1}^{(1)} - u_{v-1}^{(1)}\right) = \alpha\left[\left(u_{v+1}^{(0)} - u_v^{(0)}\right)^2 - \left(u_v^{(0)} - u_{v-1}^{(0)}\right)^2\right]. \tag{23}$$

In the right-hand side of (23) the terms appear containing various combination frequencies $\omega_p \pm \omega_n$. If one or several such frequencies coincide with the eigenfrequencies of the homogeneous equation for $u_v^{(1)}$, which are simply ω_n, these modes will be resonantly amplified during excitation. Let us find the resonance conditions by representing the difference of two frequencies in the form

$$\omega_p - \omega_n = 2\omega_{\max} \sin\left(\frac{p-n}{2N+1}\frac{\pi}{2}\right) \cos\left(\frac{p+n-1}{2N+1}\frac{\pi}{2}\right). \tag{24}$$

For the right-hand side to be equal to some eigenfrequency, p and n should have different parities, and the equality

$$2\cos\left(\frac{p+n-1}{2N+1}\frac{\pi}{2}\right) = 1 \tag{25}$$

should be fulfilled.

Because $p, n \leqslant N$ it follows from (25) that $3(p+n-1) = 2(2N+1)$, which is possible only if $2N+1$ is divisible by 3. For example, when $N=4$ and $N=7$ (for which the experimental data are available), according to (25), the resonance conditions have the form

$$\text{for } N=4 \quad \omega_4 = \omega_3 + \omega_1; \qquad \text{for } N=7 \quad \omega_4 = \omega_7 - \omega_3, \ \ \omega_5 = \omega_6 - \omega_1. \tag{26}$$

Note that, if $2N+1$ is not divisible by 3, the resonance conditions can be fulfilled approximately. Thus,

$$\text{for } N=5 \quad 2\omega_2 - \omega_4 = 0.01\omega_{\max}, \quad \omega_5 - (\omega_4 + \omega_1) = 0.02\omega_{\max}; \tag{27}$$

$$\text{for } N=6 \quad \omega_5 - (\omega_4 + \omega_1) = 0.015\omega_{\max}; \tag{28}$$

$$\text{for } N=9 \quad \omega_5 - (\omega_4 + \omega_1) = 0.008\omega_{\max}, \quad \omega_8 - (\omega_4 + \omega_3) = -0.003\omega_{\max}. \tag{29}$$

One can see that modes with subscripts 4 and 5 are present in all the cases. Therefore, it becomes clear why the best agreement with the experimental data [13] is achieved by assuming that the fourth and fifth modes play the main role in the process [26, 27].

It follows from (25) that the number of resonances increases with increasing N. For example, when $N=10$, there exist three exact resonances, although they are realised for modes with large subscripts. The resonances overlap with increasing film thickness due to their broadening, and the film acquires the properties of a bulky sample. In this case, the sound speed becomes insensitive to the film thickness.

We already mentioned that in the case of four atomic layers, the minimum frequency was observed experimentally. However, the frequencies ω_3 and ω_4 satisfying the resonance conditions (26) were not observed. We explain this by the fact that the probe-pulse duration was ~ 150 fs, and vibrations with frequencies exceeding the inverse duration of the pulse, i.e., of the order of 6–7 THz were averaged and could not be detected. In films seven atomic layers thick and thicker, a great number of incommensurable frequencies are overlapped, resulting in irregular beats.

We assume that in experiments with metals that are heavier than nickel, for example, gold, the higher-frequency phonon modes will be observed, confirming the validity of the approach discussed above.

7. Application of the FPPW method in superconductivity studies

The development of the FPPW method shows promise that precision measuring of the electron – phonon coupling

constant g in metal films will make a fundamental contribution to the physics of superconductivity [28-30].

The application of this method for studying bulky samples involves great problems, which are avoided in the case of ultrathin films. The case in point is that the penetration depth of light inside a metal is of the order of 12–15 nm, and the perturbation caused by light rapidly dissipates in the sample due to diffusion. In this case, the effects being studied have no time to manifest themselves.

Bardeen and Frohlich showed [31] that the effective matrix element of scattering of two electrons can described an exchange by a virtual phonon, which, can lead, under certain conditions, to the attraction, producing a superconducting state. It is known that the electron–phonon interaction perturbs the state of the electrons with energies lying within a narrow layer near the Fermi level. If the energy transferred from one electron to another during a scattering event is lower than the Debye energy ($\hbar\omega < \hbar u k_0$), then the scattering amplitude becomes positive, which means that the electrons are attracted to each other:

$$\Gamma = -\frac{w^2 k_0^2}{\rho(w^2 - u^2 k_0^2 + \mathrm{i}0)}, \tag{30}$$

where $\hbar\omega$ is the transferred energy; $\hbar k_0$ is the transferred momentum; u is the sound speed; w^2 is a constant proportional to the square of the matrix element of the electron–phonon interaction; and ρ is the equilibrium density of a medium. Note that it is the exchange by virtual phonons that causes the attraction between the electrons accompanied by the formation of Cooper pairs. It is obvious that the exchange by real phonons can result only in repulsion between the electrons, as follows from the law of conservation of momentum.

On the other hand, the relaxation of hot electrons due to energy transfer from the electrons to the lattice is described as emission of real phonons by electrons. Therefore, the superconductivity equations consider the exchange by virtual phonons only, whereas the TTM equations deal with emission of real phonons. To determine the electron–phonon interaction constant in the superconductivity theory from the experimental data on the relaxation of hot electrons, it is necessary to find the relation between parameters entering the TTM equations and the superconductivity theory. This problem was solved by Allen [32], and subsequent experiments confirmed the validity of his conclusions [13]. Allen showed that the constant g entering the TTM equations (2)–(4) can be expressed in terms of the second moment of the electron–phonon spectral function $a_c^2 F(\Omega)$, which is proportional to the probability of emission of a phonon with frequency Ω by an electron, as

$$g = \frac{3\hbar\lambda\langle\omega^2\rangle}{\pi k_B T_e}, \tag{31}$$

where

$$\lambda\langle\omega^2\rangle = 2\int_0^\infty \Omega^2 \left[\frac{a_c^2 F(\Omega)}{\Omega}\right] \mathrm{d}\Omega;$$

k_B is the Boltzmann constant and a_c is a constant. Expression (31) was confirmed in a number of experiments; the measured values of g were compared with those obtained by using the calculated values of the parameter $\lambda\langle\omega^2\rangle$. The agreement for gold and aluminium was satisfactory within ±30 % [13, 15]. Note that it was assumed implicitly in the papers cited in this section that the electron–phonon interaction in films and bulk samples is identical. It seems that the consideration of size quantisation of the phonon spectrum would improve the agreement, especially, for very thin films.

8. Conclusions

Femtosecond laser pulses are an efficient tool for studying ultrafast processes in solids. Such studies became very important in recent years due to the discovery of unique physical properties of low-dimensional systems such as ultrathin films, ultrathin wires, and nanoparticles. The application of such systems in ultrafast electronics requires the knowledge of their parameters with a high precision. At present, such a precision of measuring relaxation and optical constants can be achieved only by the FPPW method. Moreover, this method allows one to study the dynamics of thermal expansion of ultrathin films, which is hardly probable to do by conventional methods.

Most of the results described in the paper stimulate the continuation of studies. This concerns especially the measurement of the dependences of the film parameters of its thickness because these dependences directly affect the operation of devices. We have shown already that the size quantisation of the phonon spectrum or, in other words, phonon trapping in ultrathin metal films not only reduces the electron–phonon relaxation time but also substantially reduces the propagation velocity of a thermal expansion pulse – the sound speed in the film. We can hope that a further development of the femtosecond technique with allow us to discover new properties of low-dimensional metal structures, which, being of the fundamental interest, expand the scope of applications of these structures.

References

1. Esley G.L. *Phys. Rev. Lett.*, **51**, 2140 (1983).
2. Fujimoto J.G., Liu J.M., Ippen E.P., Bloembergen N. *Phys. Rev. Lett.*, **53**, 1837 (1984).
3. Esley G. L. *Phys. Rev. B*, **33**, 2144 (1986).
4. Elsayed-Ali H.E., Norris T.B., Pessot M.A., Mourou G.A. *Phys. Rev. Lett.*, **58**, 1212 (1987).
5. Brorson S.D., Fujimoto J.G., Ippen E.P. *Phys. Rev. Lett.*, **59**, 1962 (1987).
6. Elsayed-Ali H.E., Juhasz T., Smith G.O., Bron W.E. *Phys. Rev. B*, **43**, 4488 (1991).
7. Fann W.S., Storz R., Tom H.W.K. *Phys. Rev. B*, **46**, 13592 (1992).
8. Juhasz T., Elsayed-Ali H.E., Smith G.O., Suarez C., Bron W.E. *Phys. Rev. B*, **48**, 15488 (1993).
9. Sun C.K., Vallee F., Aciolo L.H., Ippen E.P., Fujimoto J.G. *Phys. Rev. B*, **50**, 15337 (1994).
10. Suarez C., Bron W.E., Juhasz T. *Phys. Rev. Lett.*, **75**, 4536 (1995).
11. Hohlfeld J., Müller J.G., Wellershoff S.S., Matthias E. *Appl. Phys. B*, **64**, 387 (1997).
12. Bonn M., Dencler D.N., Funk S., Wolf M., Wellershoff S.-S., Hohlfeld J. *Phys. Rev. B*, **61**, 1101 (2000).
13. Hohlfeld J., Wellershoff S.-S., Guedde J., Conrad U., Jaehnke V., Matthias E. *Chem. Phys.*, **251** (1–3), 237 (2000).
14. Kaganov M.I., Lifshitz I.M., Tanatarov L.V. *Zh. Eksp. Teor. Fiz.*, **31**, 232 (1956).
15. Tas G., Maris H.J. *Phys. Rev. B*, **49**, 15046 (1994).

16. Pines D., Nozières P. *The Theory of Quantum Liquids* (New York: W.A.Benjamin, 1966).
17. Melikyan A., Minassian H., Guerra A. III, Wu W. *Appl. Phys. B*, **68**, 411 (1999).
18. Shah J. *Hot Carriers in Semiconductor Nanostructures: Physics and Applications* (New York: Academic Press, 1992).
19. Ridley B.K. *Rep. Progr. Phys.*, **54**, 169 (1991).
20. Avetisian S.K., Melikyan A.O., Minassian H.R. *J. Appl. Phys.*, **80**, 301 (1996).
21. Alivisatos A.P. *Science*, **271**, 933 (1996).
22. Woggon U. *Optical Properties of Semiconductor Quantum Dots* (Berlin: Springer, 1997).
23. Whang E.-K., Oh J., Kim S.-K., Kim J.-S., Lee G. *Phys. Rev. B*, **63**, 075401 (2001).
24. Melikyan A., Minassian H. *Chem. Phys. Lett.*, **331** (2 – 4), 115 (2000).
25. Kittel C. *Introduction to Solid State Physics* (New York: Wiley, 1976; Moscow: Nauka, 1978).
26. Melikyan A., Minassian H. *Sol. State Commun.*, **119** (8 – 9), 497 (2001).
27. Melikyan A., Minassian H., in *Femtochemistry and Femtobiology: Ultrafast Dynamics in Molecular Science* (Singapore: World Scientific, 2002).
28. Hohlfeld J., Grosenick D., Conrad U., Matthias E. *Appl. Phys. A*, **60**, 137 (1995).
29. Sun C.K., Vallée F., Acioli L., Ippen E.P., Fujimoto J.G. *Phys. Rev. B*, **48**, 12365 (1993).
30. Corcum P.B., Brunel F., Sherman N.K., Srinivasan-Rao T. *Phys. Rev. Lett.*, **61**, 2886 (1988).
31. Landau L.D., Lifshitz E.M. *Statistical Physics, Part 2* (Oxford: Pergamon Press, 1980; Moscow: Nauka, 1976).
32. Allen P.B. *Phys. Rev. Lett.*, **59**, 1460 (1987).